Highly Thermally Conductive Polymer Composite Originated from Assembly of Boron Nitride at Oil Water Interface

Journal:	*ACS Applied Materials & Interfaces*
Manuscript ID	am-2019-15259q.R1
Manuscript Type:	Article
Date Submitted by the Author:	15-Oct-2019
Complete List of Authors:	Wang, Rui; Hefei Institutes of Physical Science Institute of Applied Technology Cheng, Hua; Hefei Normal University, Department of Chemistry and Chemical Engineering Gong, Yi; Hefei Institutes of Physical Science Institute of Applied Technology, Wang, Fengyu; Hefei Institutes of Physical Science Institute of Applied Technology Ding, Xin; Institute of Solid State Physics Chinese Academy of Sciences, Key Laboratory of Materials Physics, Hu, Rui; Institute of Applied Technology, Hefei Institutes of Physical Science, Chinese Academy of Sciences, Zhang, Xian; Chinese Academy of Sciences, Institute of Applied Technology, Hefei Institutes of Physical Science He, Jianying; Norges teknisk-naturvitenskapelige universitet, Tian, Xingyou; Institute of Solid State Physics Chinese Academy of Sciences,

Highly Thermally Conductive Polymer Composite Originated from Assembly of Boron Nitride at Oil Water Interface

Rui Wang [a, b, c], *Hua Cheng* [a, b, c, d], *Yi Gong* [*a, c], *Fengyu Wang* [a, c], *Xin Ding* [a, c], *Rui Hu* [a, c], *Xian Zhang* [a, c], *Jianying He* [e], *Xingyou Tian* [*a, c]

[a] Institute of Applied Technology, Hefei Institutes of Physical Science, Chinese Academy of Sciences, Hefei 230088, People's Republic of China

[b] University of Science and Technology of China, Hefei 230026, People's Republic of China

[c] Key Laboratory of Photovolatic and Energy Conservation Materials, Chinese Academy of Sciences

[d] Department of Chemistry and Chemical Engineering, Hefei Normal University

[e] Department of Structural Engineering, Faculty of Engineering, Norwegian University of Science and Technology (NTNU), 7491, Trondheim, Norway

Keywords: Oil-water interface; Boron nitride; Thermal conductivity; Thermally conductive polymer; Polystyrene

ABSTRACT Thermally conductive polymer packaging material is of great significance for the thermal management of electronics. Inorganic thermally conductive fillers have been demonstrated as a convenient approach to achieve this goal, however, sacrificing the lightweight and processability of the polymer. To address this problem, effective 3D boron nitride (BN) network was constructed as heat conduction pathway in polystyrene (PS) matrix based on oil-water interface assembly in this work. Styrene oil droplets were stabilized by BN sheets in water phase to form Pickering emulsions, and then the *in-situ* polymerization was trigged to synthesize PS microspheres with ultrathin BN layer covered surface (PS@BN microspheres). Composite substrates were fabricated through hot-compressing the PS@BN microspheres to form BN networks based on the original microsphere template. Benefited from the network structure, the maximum thermal conductivity of composite substrate reached 0.94 W/mK at 33.3 wt% BN, which is 626% folds of that of pure polystyrene. It was also demonstrated that the storage modulus and thermal stability of the composite substrate were dramatically improved by the BN network. The reported composite substrate and its fabrication strategy are promising in the development of thermal management of electronics.

1. Introduction

With the fast development of the electronics industry, power density of the electronics increases rapidly, resulting in severe heat accumulation problems. Insufficient heat dissipation performance of electronic packaging materials seriously threatens the working stability and lifespan of electronic products.[1-6] Polymers currently hold an absolutely dominant share in electronic packaging materials due to their electrical insulation, low cost, facile processability, and lightweight. However, the inherent thermal conductivity of polymer materials is rather low, only about 0.1-0.3 W/mK, which is difficult to meet the heat dissipation requirements of electronic packaging materials.[7-12] Therefore, development of polymer material with high thermal conductivity is on urgent demand.

Introduction of thermally conductive fillers such as boron nitride (BN), aluminum oxide, carbon, is a promising method to improve the thermal conductivity of polymer matrix.[13] However, it is still a huge challenge to optimize the distribution of thermally conductive fillers in the polymer matrix to form an effective heat conduction pathway.[3, 11, 14, 15] Three-dimensional (3D) networks of thermally conductive fillers have been proven as an efficient structure for thermal conductivity enhancement of polymer matrix. Various methods for construction of 3D thermally conductive networks have been developed based on the assembly of the fillers. The techniques for filler assembly could be roughly classified as following: (1) **Chemical modification enabled assembly**.[3, 16, 17] Strong interaction between the filler and polymer is introduced through chemical modification, guiding the assembly of the

filler to form thermally conductive networks. For example, Gu et al. reported that the NH_2-POSS functionalization of BN fillers increased the thermal conductivity coefficient of BN/polyimide composites from 0.69 W/mK to 0.71 W/mK at 30 wt% BN content.[18] Jiang et al. reported thermally conductive BN network construction based on hydrogen bond between hydroxy modified BN particles and polyvinyl alcohol.[3] (2) **External field assisted assembly.**[19-21] Magnetic field regulated self-assembly of the magnetic filler is an efficient method to form network. Our group previously reported that the orientations of iron oxide modified magnetically responsive BN could be controlled by external magnetic field in polymer matrix, obtaining a 3D interconnected network of BN platelets and carbon nanotubes.[13] (3) **Phase separation induced self-assembly**. Phase separation such as icing[22] or other crystallization[23] caused nucleation from homogeneous solution, which provided template for the assembly of the fillers. Hu et al. reported 3D-BN network from ice-templating self-assembly of BN, epoxy composites was then fabricated as thermal interfacial materials by infiltration technology.[22] (4) **Microsphere template assisted assembly.**[8, 24-28] Thermally conductive fillers and microspheres are physically mixed at the beginning, further processing such as hot-compression will be applied to convert the microspheres into polymer matrix, forming polymer matrix with thermally conductive filler network. Wang et al.[8] reported that BN nanosheets and PS microspheres formed composite microspheres *via* strong electrostatic interactions for the thermal interface material fabrication based on latex blending and subsequent compression molding. Our group demonstrated that porous silicon carbide nanowires

(SiCw) skeleton could be formed based on polystyrene microspheres templates and epoxy-based composites with structurally segregated SiCw manufactured after sintering and infiltrating.[25]

Water-oil interface is a desired platform for the self-assembly of colloidal/nano particles. For example, Pickering emulsions are kinetically stabilized by solid particles instead of surfactant.[29, 30] Pickering emulsions, stabilized by 2D materials such as graphene oxide, BN nanosheets,[31] have been widely reported and Pickering emulsion could be employed as soft templates for the preparation of functional hybrid materials.[30, 32-35] Among other 2D materials, BN shows excellent thermal conductivity, good electrical insulation and low dielectric constant,[36-38] which was highly desirable for the electronic packaging materials.

In this work, self-assembly of BN at water/styrene interface was employed to prepare BN-coated PS (PS@BN) microspheres by *in-situ* emulsion polymerization. PS@BN microspheres were hot-compressed into composite substrates and thermal conductivity and mechanical properties of which were investigated. To the best of our knowledge, this work is the first time to propose emulsion templet method in the field of thermally conductive filler network construction. Compared to the reported methods in the literatures, assembly of BN on emulsion templet offers an ultrathin layer of close packed BN network in polymer matrix, enabling highly thermally conductive composite PS substrate. The proposed preparation method also avoids any surfactants or chemical modification, which is a facile and green route for the fabrication of functional materials. The explored relation between

the BN distribution in matrix and thermal/mechanical properties of composite substrate will shed new light on the design of electronic packaging polymers.

2. Materials and experiment

2.1 Materials

BN particles (Chemical Abstracts Service Registry Number (CAS No.) : 10043-11-5, purity： 98.5%, average diameters： 1 μm) were provided by Shanghai Macklin Biochemical Co., Ltd. BN particles (CAS No. : 10043-11-5; purity： 98%, average diameters： 3 μm and 5 μm) were provided by Dandong Rijin Science and Technology Co., Ltd. Sodium hydroxide (CAS No.:1310-73-2, purity: ≥ 96.0％) was purchased from Sinopharm Chemical Reagent Co., Ltd. Styrene (CAS No.:100-42-5, Analytical Reagent (AR), supplied by Shanghai Aladdin biochemical Co., Ltd) was washed by 5 wt% of sodium hydroxide solution before use. Benzoyl peroxide (CAS No.: 94-36-0, AR) was purchased from Shanghai Aladdin biochemical Co., Ltd. Deionized water was purified by the Milli-Q water purification system.

Table 1. The recipe of the Pickering emulsion for the preparation of PS@BN microspheres

Sample name	Weight of BN (g)	BN ratio in the Feed (wt%)
PS@BN -9.09%	2.0	9.09
PS@BN -14.9%	3.5	14.9
PS@BN -25.9%	7.0	25.9
PS@BN -33.3%	10.0	33.3

2.2 Preparation of Pickering emulsion

0.20 g of benzoyl peroxide was dissolved in 20.0 mL of styrene to form an oil phase. The specified amount of the BN powder in the Table 1 was dispersed in 200.0 mL deionized water. The mixture of BN and water was sonicated for 30 min to obtain uniform water dispersion. The water dispersion and oil phase were mixed and emulsified with the aid of emulsification machine (FLUKO, Germany) for 2 min at the rotating speed of 10000 rpm. Then a stable Pickering emulsion was obtained.

2.3 Preparation of PS@BN microspheres

The as-formed Pickering emulsion was transferred into a 500 mL three-neck round bottom flask. Nitrogen was introduced to the flask to replace the air for 30 min, then the flask was placed into a 70 ℃ water bath to trigger the *in-situ* polymerization. The polymerization lasted for 10 hours without any stirring. The products were collected by centrifugation at 9000 rpm and the precipitate was washed by ethanol for 4~5 times to remove the excessive styrene monomer. The products were dried in vacuum oven at 40 ℃ for 24 hours. The obtained composites were named as PS@BN microspheres.

2.4 Preparation of composite substrate

The composite substrates were prepared with the aid of Hot-compressing Machine (WuHan QiEn Science and Technology Development Co., Ltd, China). 3.0 g PS@BN microspheres were placed in a mould (25 mm×25 mm×2 mm). The mould was preheated to the investigated temperature (80 ℃ or 95 ℃) and the sample inside was compressed at certain pressure (10 MPa or 25 MPa) for 15 min. The composite was formed after another pressing for 5 min when the whole system was cooled to 25 ℃.

2.5 Characterization

Pickering emulsions were observed with an optical microscope (Olympus BX53, Japan). The morphology of PS@BN and cross-section of composites substrate were examined by scanning electron microscopy (SEM, Sirion-200 FEI, America). The element distribution of the samples was investigated by the energy dispersive spectroscopy (EDS) detector equipped in SEM. The size distribution of PS@BN microspheres was obtained from statistics based on counting over 200 samples with the aid of the software Nanomeasurer. The XRD (X-ray diffraction) analyses of BN and PS@BN were carried out with a Philips X' Pert Pro MPD X-ray diffractometer with Cu Kα radiation (λ = 0.154 nm, 40 kV, 40 mA). The thermal stabilities of the composites were studied by Thermogravimetric Analysis (TGA, Perkin-Elmer, USA, Pyris1) from 20 to 900 ℃ at a heating rate of 10 ℃/min in air atmosphere. The thermal conductivity of composite substrate was measured by Hot Disk instrument (TPS 2200, AB Corporation, Sweden) in isotropic mode. The storage modulus and loss factor (tanδ) of composite substrate were performed on a dynamic mechanical analyzer (Diamond DMA, Perkin-Elmer, USA). The samples were tested from room temperature to 150 ℃ with a heating rate of 2 ℃/min and a testing frequency of 1 Hz. The composite substrate was heated from 25 ℃ to 70 ℃ placed on a homemade programmable point heating device and a Handheld infrared camera (CEM DT-980, Huashengchang, China) was applied to visualize the temperature distribution evolution of the substrate during this process. 5 μL deionized water or styrene was added on a BN tablet (diameter: 12.5 mm, thickness: 1.5 mm) made from

compressing the BN powder, and the contact angle of the droplet was measured by Data Physics optical Contact Angle (CA-100&D, Shanghai Innuo Precision Instruments Co., Ltd, China). The stability of emulsion was assessed by emulsion stability index (ESI). The ESI was measured by the height of the separated oil phase relative to the height of the remaining emulsion, which was calculated as the percentage ratio of the emulsion height to the sum of the emulsion height plus the height of separated oil phase[39]. The X-ray photoelectron spectra (XPS) was performed on ESCALAB 250 (Thermo-VG Scientific) for analyzing the elemental compositions at the surface of samples.

3. Results and discussion

3.1 Formation of Pickering Emulsion

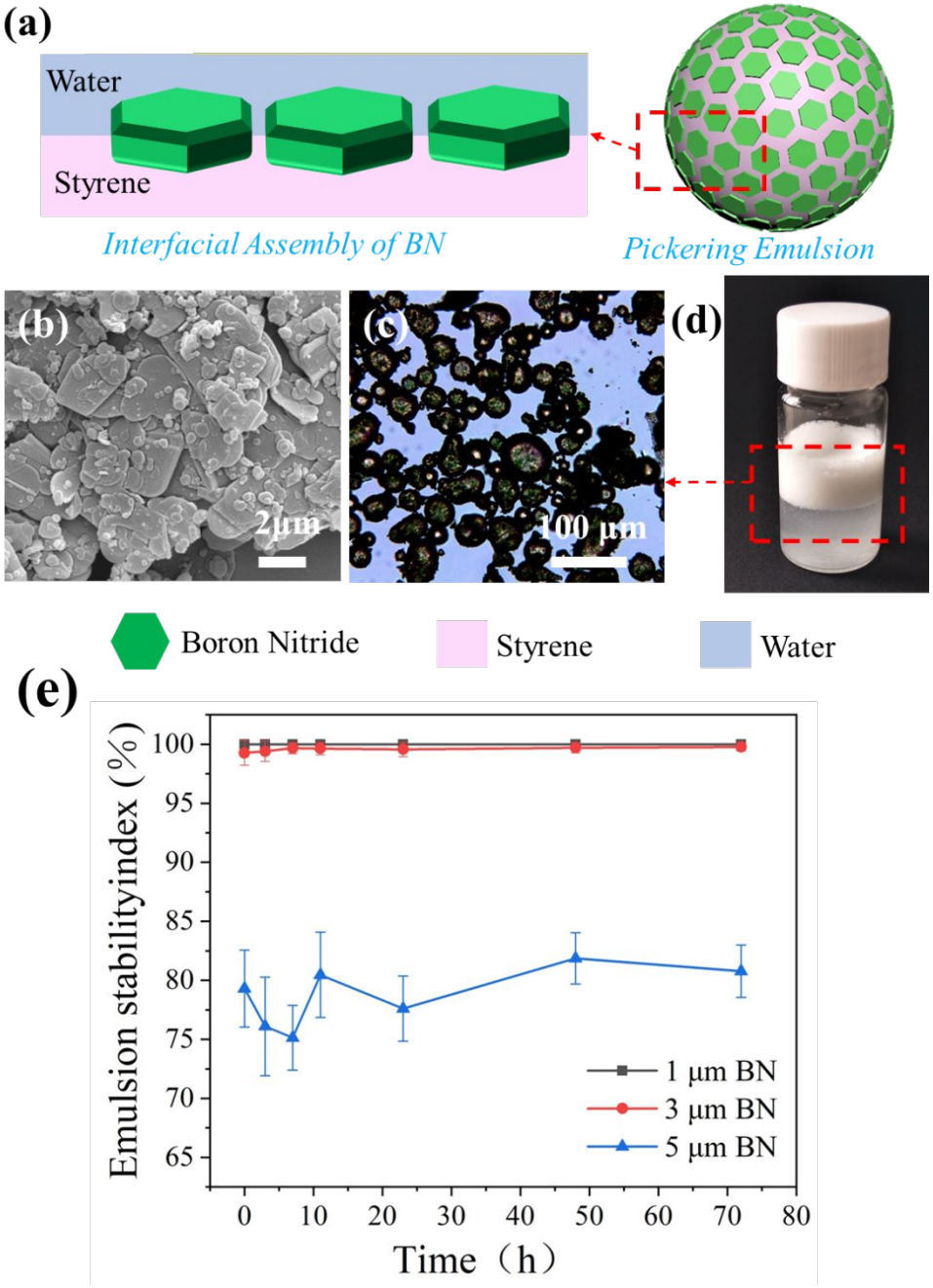

Fig. 1 (a) Schematic of Pickering emulsion, (b) SEM image of BN particles with mean size of 3 μm (c) the optical microscopy image of Pickering emulsions; (d) photograph of typical Pickering emulsion stabilized by BN； and (e) Emulsion stability index (ESI) as a function of time for Pickering emulsion stabilized by BN particles.

The process of Pickering emulsion formation is schematically described in Fig. 1a. The oil and water phases were sufficiently emulsified at the 10000 rpm. Due to the massive shear force from the emulsification, a large area of bare oil-water interfaces was created. These bare oil-water interfaces were energetically unfavorable, tending to adsorb BN particles (Fig. 1b and Fig. S2 in the supporting information) for the free energy minimization of the system. As a result, the as formed emulsions were stabilized by BN particles in the form of that a layer of the BN particles were adsorbed at the oil-water interface. The emulsion droplets ranging from several micrometers to several tens of micrometers were observed from the optical microscope image (Fig. 1c). The dark edge of the emulsion droplets confirmed that the emulsion was stabilized by the opaque BN sheets. The density of the oil phase (styrene) is 0.906 g/mL at 20 °C, which is lower than that of water, thus the obtained milky oil-in-water emulsion floated above the transparent water phase (Fig. 1d) after a short period of standing. Emulsion stabilized by 1 μm and 3 μm BN showed excellent stability based on the ESI in Fig.1e, indicating that the emulsion is stable during the 10 hour polymerization. In contrast, the emulsion stabilized by 5 μm BN exhibited a low ESI with large fluctuation. The photographs of emulsion evolution were shown in Fig. S1 in Supporting Information, where obvious oil phase separation could be found in emulsion stabilized by 5 μm BN.

3.2 Preparation of PS@BN composite microspheres

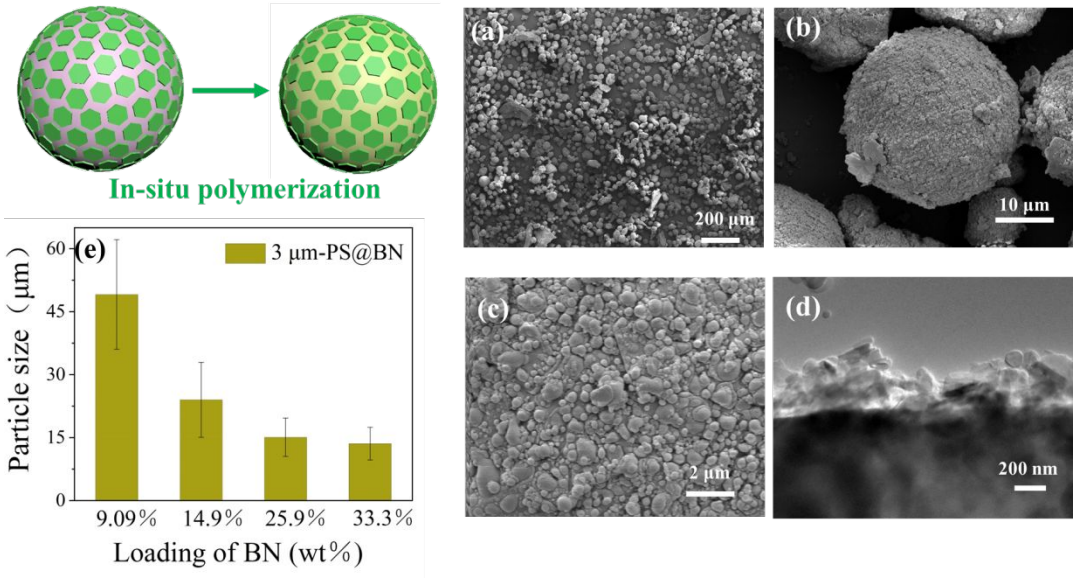

Fig. 2 The cartoon illustrates the formation of PS@BN microspheres from *in-situ* polymerization of Pickering emulsion. (a) SEM image of PS@BN microspheres stabilized by 3 μm BN sheets. SEM images of a typical PS@BN microsphere with (b) low and (c) high magnifications; (d) TEM image, (e) particle size distribution

PS@BN composite microspheres were fabricated by the *in-situ* polymerization of styrene monomer in the emulsion. The solubility of the initiator determined polymerization position. The water-soluble initiator ammonium persulfate (APS) could start the polymerization of the diffused styrene in water phase, leading to PS microspheres without any BN coating (Fig S3 in Supporting Information). The oil-soluble benzoyl peroxide (BPO) was employed in this study to achieve an emulsion template polymerization. BPO was dissolved in the monomer in the separated phases in the emulsion. The polymerization took place inside the emulsion droplets, which were stabilized by the BN sheets, ensuring that the surface of the formed PS microspheres was covered by BN sheets. The obtained microspheres

exhibited a uniform size distribution with an average diameter around several tens of microns (Fig. 2a and 2b), that was consistent with the mean diameter of emulsion droplets observed by optical microscopy. Compared with smooth surface of pure polystyrene microspheres (Fig. S4), PS@BN microspheres exhibited a rough surface due to the coexistence of BN sheets and PS structure (Fig. 2c). The thickness of the BN layer was less than 1 micrometer according to the TEM image (Fig. 2d). This is because that only the BN adsorbed at the oil-water interface could be anchored at the surface of PS microspheres. This ultrathin BN layer raised the possibility for achieving high thermal conductivity in relatively low BN loading, which will be discussed in the following sections. The size of the PS@BN microspheres decreased with the BN content in the feed during the polymerization (Fig. 2e). It was attributed that the increasing amount of BN sheet provided more stabilized interfaces during the emulsification. For the identical amount of oil phase, more interface area of the emulsion droplets led to smaller droplets size. It suggested that BN content could be used to control the size of the PS@BN microspheres.

3.3 Mechanism of the PS@BN microspheres formation

The formation of PS@BN microspheres relied on the BN assembly on the oil-water interface. The stability of the colloidal particles was mainly determined by the hydrophobicity and size.[40] The powder of BN sheets was compressed into tablet to investigate its wettability. Fig 3a illustrates the configuration of contact angle measurement. The tablets from BN with mean size of 1 μm, 3 μm and 5 μm BN showed a mean contact angle of 26.8 ± 0.3°, 52.3 ± 0.7° and 67.6 ± 0.5° (Fig. 3c-3e),

respectively, indicating good water wettability of BN.[41, 42] The good water wettability of BN was attributed to the -OH at surface, which was confirmed by the high-resolution XPS spectra of 3 μm BN (Fig. 3l). The peak at 190.6 eV is assigned to B-N bond while the peak at 191.3 eV is assigned to the B-O bond (Fig. 3m).[43-45] The -OH on the BN also could be observed from the FTIR spectrum (Fig. S4). All the contact angles of styrene droplets on the tablets made from different sized BN sheets were closed to 0° in Fig. 3f-3h, indicating a strong interaction between BN and styrene. It was attributed to that delocalized electrons from hexagonal BN and the aromatic structure of styrene formed a strong, noncovalent bond *via* π-π stacking (Fig 3b) and van der Waals interactions.[12, 46, 47] Since BN sheets could be wet by both water and styrene, they were able to firmly anchor at the interface. After the polymerization in the oil droplets, the interfacial BN sheets were bonded to the PS microsphere, as shown in Fig 2d.

The desorption energy of BN from the interface increases with its size, indicating that the increasing BN size improved the stability of the emulsion (Fig.S1a-b). However, the gravitational force gradually played an important role, promoting the desorption of BN from the interfaces. Composite microspheres prepared from BN sheets with average size of 1 μm and 3 μm as stabilizer (Fig. 3i and 3j) showed spherical morphology with desired BN and PS distribution. Further increase of BN size led to BN attached anomalistic particles mixed with irregularly shaped fragments (Fig. 3k). The phenomenon indicated that emulsion showed less stability when it was stabilized by BN nanosheets with average size

larger than 5 μm (Fig.S1c.)

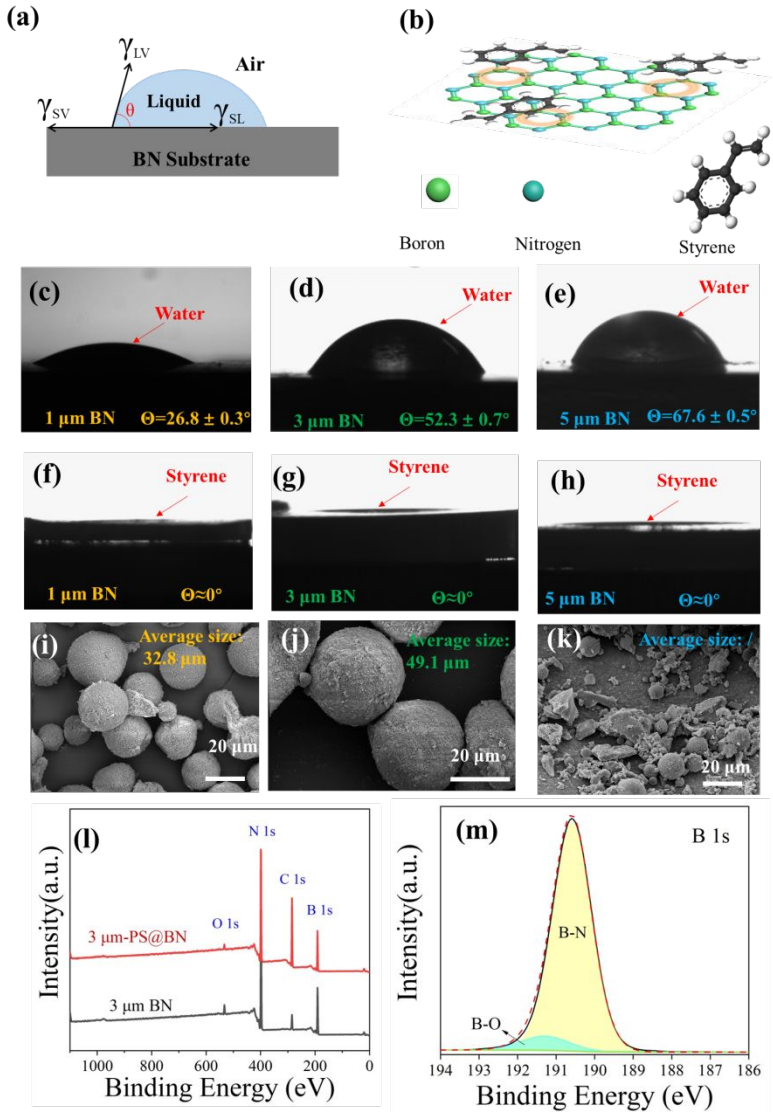

Fig.3 (a) Schematic configuration of contact angle measurements; (b) schematic illustration of interaction between BN and PS, the orange ring denotes the π-π stacking effects; (c-e) contact angles of water droplet on the tablets made of BN with various sizes; (f-h) contact angles of styrene droplet on the tablets made of BN with various sizes; SEM images of PS@BN microsphere obtained by BN sheets with mean size of (i)1 μm, (j) 3 μm and (k) 5 μm. (l) XPS spectra of the 3 μm BN and 3 μm-PS@BN microspheres; (m) B 1s high-resolution spectrum of 3 μm BN . The content of BN in feed was 9.09 wt% for the preparation of all the above samples.

3.4 Preparation of composite substrate

The composite substrates were prepared by hot-compressing the PS@BN microspheres. The DSC (Fig. S5) curves suggested that the glass transition temperature of the PS@BN was between 90.5 - 93.3 ℃. The fluidity of PS increased above the glass transition temperature and PS@BN microspheres would merge together to form the composite substrate under physical pressure. Pores between the microsphere units in the cross-section of composite substrate (Fig. 4c) were observed for the sample hot-compressed at 80 ℃, 25 MPa, indicating incomplete contact between the BN and PS matrix. When the temperature of hot-press reached to 95 ℃, PS microspheres merged into a complete polymer matrix while BN located at the interfaces of the original microspheres, forming a three-dimensional network (Fig. 4d). Fig. 4a-4b showed the Carbon (C) and Nitrogen (N) element distribution at the surface of PS@BN composite microspheres and cross-section of composite substrate. The C and N elements maps complementary with each other, indicating BN and PS were co-existed on the surface of the microspheres. After hot-compressing, ultra-thin network of Nitrogen element (Fig. 4b) was observed in the PS matrix. The X-ray diffraction peaks (Fig. 4f) of the composite substrate at approximate 26.7° and 41.3° were associated with the (002) and (100) planes of BN, respectively. The compression could cause the re-orientation of the BN in the polymer matrix, according to the literature, in which the value of I(002)/I(100) could reach 1057.[48] The value of I(002)/I(100) of our composite substrate increased from 3.2 to 18.9 when the BN content was increased from 9.09 to 33.3 wt%, much smaller than that of the literature,

indicating a negligible deformation during the compression, thus the integrity of BN network could be maintained.

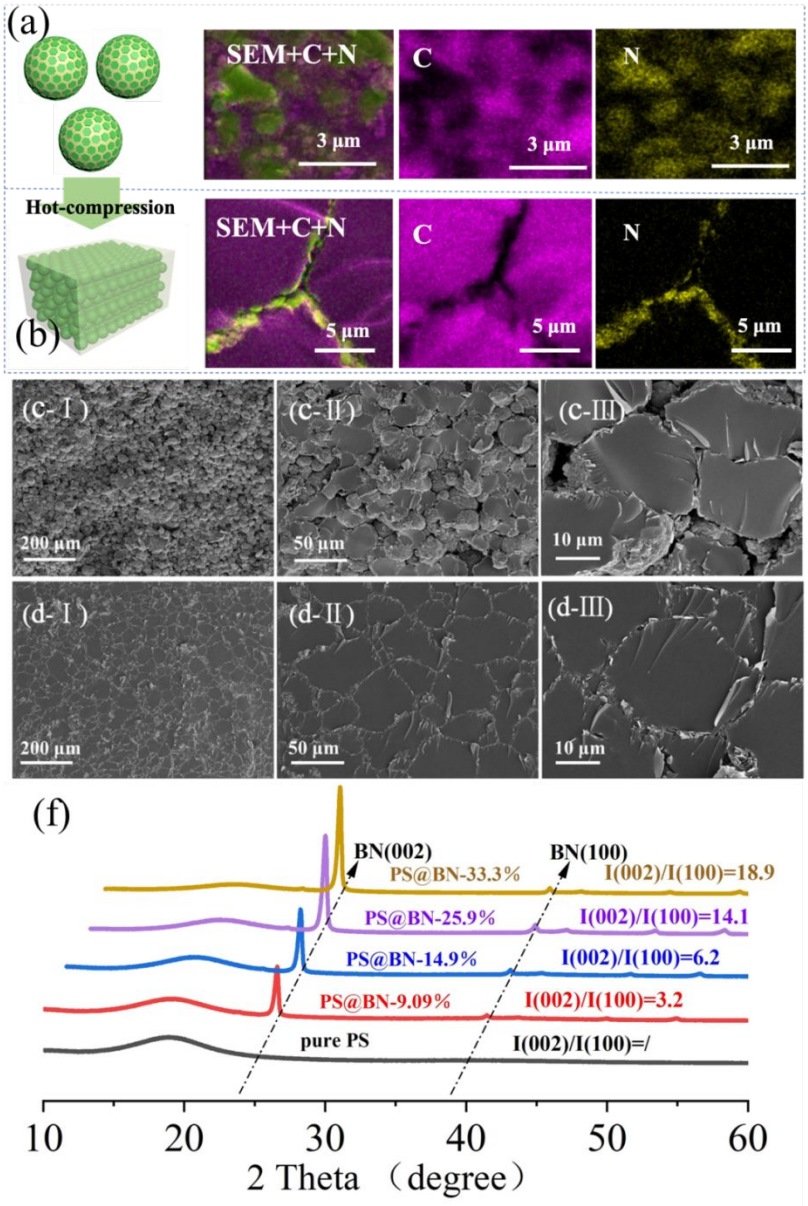

Fig. 4 EDS elemental mapping images of (a) the surface of PS@BN composite microspheres and (b) cross-section of composite substrate; cross-section SEM images of composite substrate under different conditions of hot-pressing: (c) 80℃, 25MPa; (d) 95℃, 25Mpa; Ⅰ, Ⅱ, Ⅲ represent the SEM at different magnifications,

respectively; (f) XRD patterns of the composite substrates made from PS@BN microspheres with varies BN loadings.

3.5 Mechanical properties and thermal stability of the composite substrates

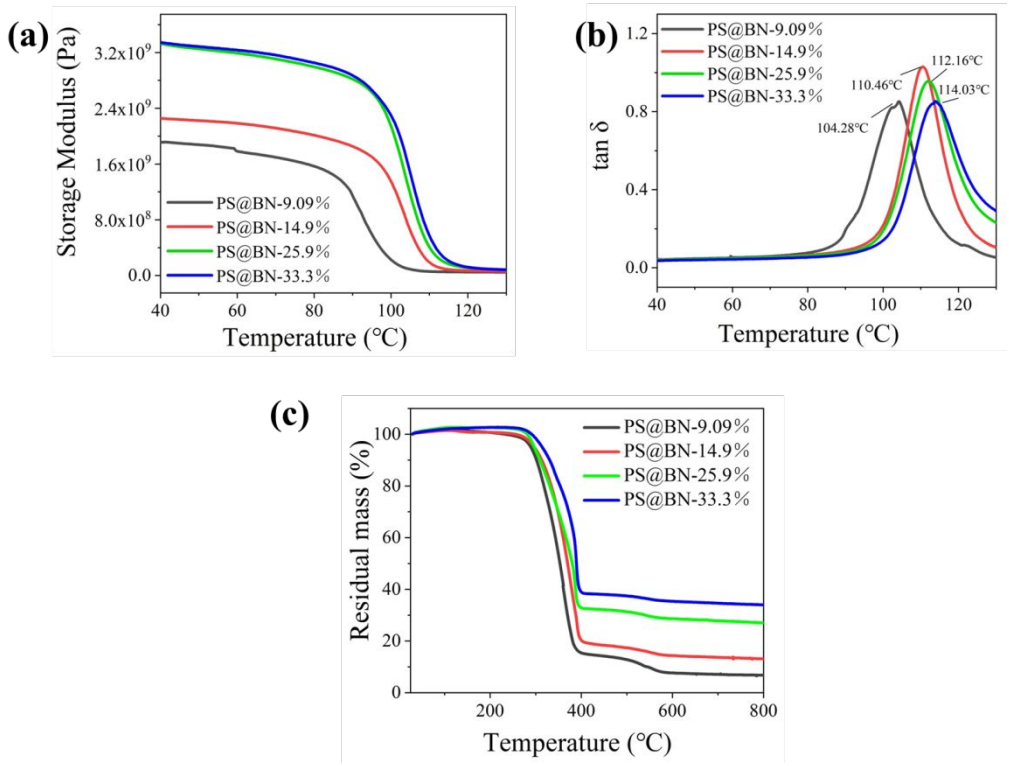

Fig. 5 Dynamic mechanical analysis (DMA) of the PS@BN composite substrates, (a) storage modulus and (b) loss tangent (tan δ) versus temperature of the composite substrates; (c) thermogravimetric analysis of PS@BN composite substrates with increased content of BN.

Distribution and volume fraction of inorganic filler in polymer matrix could affect the viscoelastic properties of polymeric materials dramatically.[2, 49] As depicted in Fig. 5a, the composite substrate with larger content of BN exhibited a higher storage modulus at the low temperature region, indicating that the mechanical strength of the substrate could be enhanced by BN. The rigidity of the polymer matrix increased due

to the blending of rigid inorganic fillers. When the temperature was higher than 120 ℃, the mobility of the polymer chains was significantly improved, limiting the role of rigid filler in the polymer matrix, thus causing a sharp drop in the storage modulus of the material.

The loss tangent (tan δ) is the ratio of loss modulus to the storage modulus. As shown in Fig. 5b, the glass transition temperature (Tg) of composite was considered to be the temperature corresponding to the peak value of tan δ.[25, 50] Tg values of PS@BN composites with 9.09 wt%, 14.9 wt%, 25.9 wt%, 33.3 wt% BN contents were 104.28, 110.46, 112.16, 114.03 ℃, respectively, shifting to higher temperatures with the increasing content of BN sheet. As the content of the rigid inorganic filler increased, the movement of the polymer segment was limited. Polymer chains required excess energy to overcome the induced resistance to achieve chain motion.[2, 51] Therefore, the glass transition temperature of the material gradually increased when increasing the filler content.

The thermogravimetric analysis curves of the composites are shown in Fig. 5c. The residual value of the composite was roughly used as the BN content, assuming that the PS was totally decomposed while the BN maintained stable during heating. The residual mass of BN was converted to a volume fraction,[52] as shown in Table S1. The thermal residual value confirmed that only part of the thermally conductive fillers was coated in PS@BN microspheres. According to Table S1 in Supporting Information, thermal decomposition temperatures at 5% of the weight loss (T5) of the composite increased with BN content, suggesting that the initial decomposition temperature of

the composites could be increased by incorporation of inorganic thermal fillers. The phenomenon indicated that thermal stability of the composite would be enhanced by gradually adding inorganic fillers. T50 stands for the thermal decomposition temperatures at 50% of the weight loss, the relation between T50 and BN loading showed similar trend with that of T5, confirming that the thermal stability of the composite could be enhanced by the BN sheets.

3.6 Thermal conductivity of the composite substrate

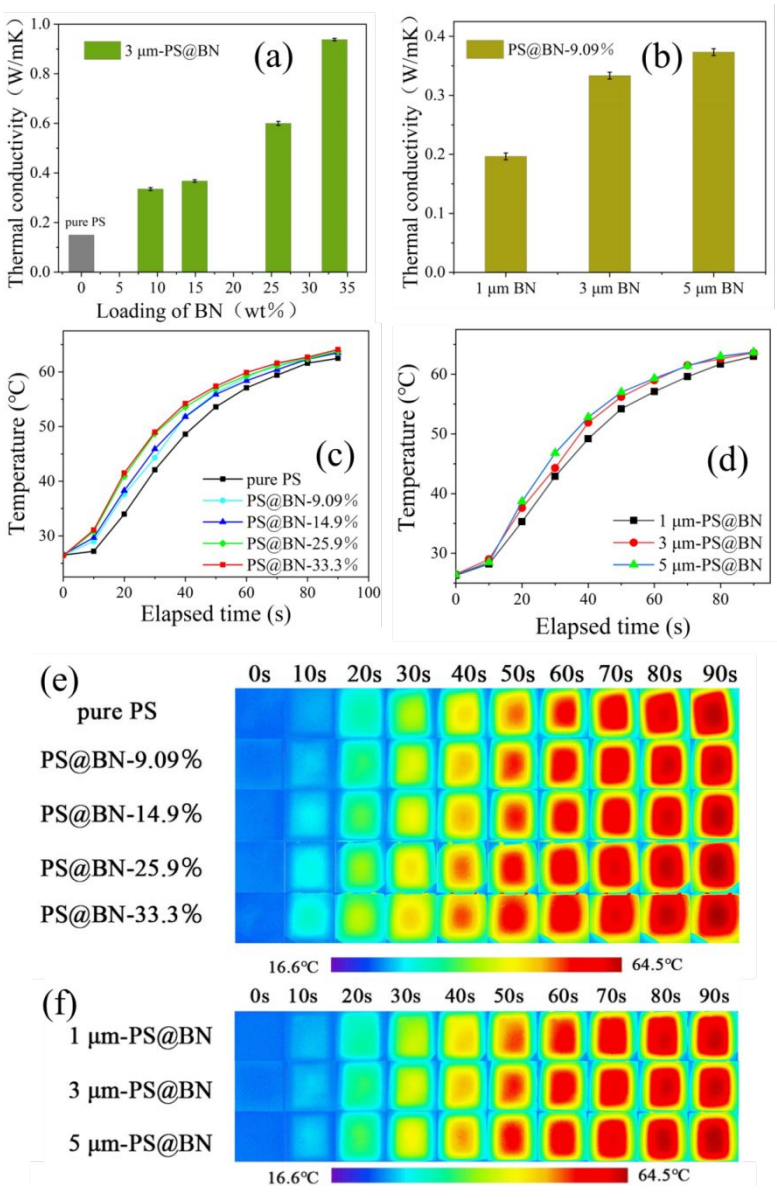

Fig. 6 (a) Thermal conductivity of composite substrate against the BN content; (b) thermal conductivity of composite substrate against the size of BN; surface temperature evolution with elapsed time of the composite made with different BN (c) loadings and (d) sizes; infrared images taken by each 10 seconds for the composite substrate made with different BN contents (e) and different BN sizes (f)

The loading ratio and the mean size of BN sheets were found to be two important factors controlling the thermal conductivity of the composite substrate. The thermal conductivity of the composite substrate was 0.38 W/mK at BN loading of 9.09 wt%, 253% improvement compared to the pure polystyrene (0.15 W/mK[53]). It was attributed to that the thermally conductive 3D BN network dramatically improved thermal conductivity of PS matrix. Thermal conductivity increased from 0.38 to 0.94 W/mK when the content of BN was lifted from 9.09 wt% to 33.3 wt% (Fig. 6a). High physical BN loading is one of the reason for the thermal conductivity enhancement, the other reason is that the mean size of the PS@BN microspheres decreased with the BN loading (Fig 2e). The smaller PS@BN microsphere led to a denser BN 3D network in the composite substrate, thereby facilitating heat transfer and improving the overall thermal conductivity of the material. Heat transportation along large sized BN experienced less interfacial thermal resistances in the composite substrate, as a result, the thermal conductivity of the composite substrate increased with BN size (Fig. 6b). It is noteworthy that even emulsion stabilized by 5 μm showed relatively low ESI and some irregular shaped composite particles could be found after the polymerization (Fig 3k). The composite microspheres made from 5 μm BN showed

highest thermal conductivity. It indicated that regardless of the imperfect shape, the surface attached BN at PS particles also could form thermally conductive network after hot-compression (Fig. 6b).

The heat conduction performance of the composite substrate was demonstrated by upside surface temperature monitoring during the downside heating. The temperature increased faster of the substrate with high BN loadings (Fig. 6c) at the beginning, agreeing well with the trend of thermal conductivity. The temperature difference gradually converged after 40s (Fig. 6c) because the heat conduction tended to reach equilibrium after a certain time. The surface temperature of composite substrate made from larger sized BN responded faster to the heating compared to that made of smaller sized BN, as shown in Fig 6d. The temperature evolution (Fig. 6e and 6f) of composite during heat showed well agreement with the results of thermal conductivity measurements, suggesting the improved heat conduction performance of the PS matrix after the introduction of BN network.

Polymer composites usually require high thermally conductive filler loadings to achieve high thermal conductivity,[3] sacrificing the advantage of the polymer such as light weight and ease processability and so on. Therefore, improving thermal conductivity of polymer at low filler content is still a challenge. This work demonstrated that composite substrate fabricated from emulsion template method is comparable to the polymer materials prepared from other recently developed methods.

Table 2 Comparison of thermal conductivity of polymer composites from recent literatures

Typical Sample	Filler loading	Thermal Conductivity (W/mK)	Filler Size (μm)	Year
BNNS/PVA	10 wt%	0.7321	1.0–2.0	2019[44]
BN@PS/(PP/PS)	About 15 wt%	About 0.45	50	2018[54]
BN/CPS	15.9 wt%	0.692	/	2016[27]
AlN/PS	25 wt%	0.418	2	2016[55]
Epoxy/BN	40 vol%	1.98	13	2019[51]
PS/BN	St/BNNS=5:1	1.1	/	2015[56]
Epoxy/BN-Al_2O_3	26.5 vol%	0.808	3	2014[57]
PS@BN	33.3 wt%	0.94	3	**This work**

4. Conclusion

In summary, a facile method for fabricating PS@BN composite microspheres from *in-situ* polymerization based on emulsion template was reported. PS substrate with embedded 3D inorganic BN network was obtained by further hot compression of PS@BN microspheres at 95 ℃. Due to the 3D thermally conductive BN network from the self-assembly of BN at oil-water interface, the BN/PS composite substrate exhibited a maximum thermal conductivity of 0.94 W/mK at BN loading of 33.3 wt%. The mechanical strength and thermal stability of the composite microspheres were also dramatically enhanced by the introduction of BN. BN network constructed from

interfacial assembly for the fabrication of potential electronic packaging material has been demonstrated.

ASSOCIATED CONTENT

Supporting Information

Stability of Pickering emulsion stabilized by BN; Morphologies of BN particles and PS microspheres; FTIR spectrum of BN particles; Differential scanning calorimetry (DSC) of PS@BN microspheres; and Thermogravimetric Analysis (TGA) of PS@BNPS@BN microspheres could be found in Supporting Information which is available free of charge.

AUTHOR INFORMATION

Corresponding Author

*E-mail: yigong@rntek.cas.cn (Yi. Gong)

*E-mail: xytian@issp.ac.cn (Xingyou. Tian)

Notes

The authors declare no competing financial interest.

Author Contributions

The authors contributed equally.

ACKNOWLEDGMENT

The authors gratefully acknowledge the financial support from the National Key Research and Development Program of China (2017YFB0406200); Science and Technology Service Network Program of the Chinese Academy of Sciences (KFJ-STS-ZDTP-069); Anhui Provincial Natural Science Foundation (1908085QB64

and 1808085QE160); CASHIPS (Hefei Institutes of Physical Science, Chinese Academy of Sciences) Director's Fund (YZJJ2019QN23); Young Teachers Special Project of Hefei Normal University (2017QN17); Key Lab of Photovoltaic and Energy Conservation Materials, Chinese Academy of Sciences; and Anhui Province Key Laboratory of Environment-friendly Polymer Materials. The Research Council of Norway is acknowledged for the grant to Project No. 251068 Engineering Metal-Polymer Interface for Enhanced Heat Transfer.

Reference:

(1) Jiang, H.; Wang, Z.; Geng, H.; Song, X.; Zeng, H.; Zhi, C., Highly Flexible and Self-Healable Thermal Interface Material Based on Boron Nitride Nanosheets and a Dual Cross-Linked Hydrogel. *ACS Appl. Mater. Interfaces* **2017,** *9* (11), 10078-10084.

(2) Yang, N.; Xu, C.; Hou, J.; Yao, Y.; Zhang, Q.; Grami, M. E.; He, L.; Wang, N.; Qu, X., Preparation and Properties of Thermally Conductive Polyimide/Boron Nitride Composites. *RSC Adv.* **2016,** *6* (22), 18279-18287.

(3) Jiang, F.; Cui, S.; Song, N.; Shi, L.; Ding, P., Hydrogen Bond-Regulated Boron Nitride Network Structures for Improved Thermal Conductive Property of Polyamide-imide Composites. *ACS Appl. Mater. Interfaces* **2018,** *10* (19), 16812-16821.

(4) Zhu, Z. Z.; Li, C. W.; Songfeng, E.; Xie, L. Y.; Geng, R. J.; Lin, C. T.; Li, L. Q.; Yao, Y. G., Enhanced Thermal Conductivity of Polyurethane Composites via Engineering Small/Large Sizes Interconnected Boron Nitride Nanosheets. *Compos. Sci. Technol.* **2019,** *170*, 93-100.

(5) Xu, S.; Cai, S.; Liu, Z., Thermal Conductivity of Polyacrylamide Hydrogels at the Nanoscale. *ACS Appl. Mater. Interfaces* **2018,** *10* (42), 36352-36360.

(6) Su, Z.; Wang, H.; Ye, X.; Tian, K.; Huang, W.; He, J.; Guo, Y.; Tian, X., Anisotropic Thermally Conductive Flexible Polymer Composites Filled with Hexagonal Boron Nitride (h-BN) Platelets and Ammine Carbon Nanotubes (CNT-NH2): Effects of the Filler Distribution and Orientation. *Composites, Part A* **2018,** *109*, 402-412.

(7) Chen, H.; Ginzburg, V. V.; Yang, J.; Yang, Y.; Liu, W.; Huang, Y.; Du, L.; Chen, B., Thermal Conductivity of Polymer-based Composites: Fundamentals and Applications. *Progress in Polymer Science* **2016,** *59*, 41-85.

(8) Wang, X.; Wu, P., Preparation of Highly Thermally Conductive Polymer Composite at Low Filler Content via a Self-Assembly Process between Polystyrene Microspheres and Boron Nitride Nanosheets. *ACS Appl. Mater. Interfaces* **2017,** *9* (23), 19934-19944.

(9) Chen, J.; Huang, X.; Sun, B.; Jiang, P., Highly Thermally Conductive Yet Electrically Insulating Polymer/Boron Nitride Nanosheets Nanocomposite Films for Improved Thermal Management Capability. *ACS Nano* **2018,** *13* (1), 337-345.

(10)Yao, Y.; Zeng, X.; Wang, F.; Sun, R.; Xu, J.-b.; Wong, C.-P., Significant Enhancement of Thermal Conductivity in Bioinspired Freestanding Boron Nitride Papers Filled with Graphene Oxide. *Chemistry of Materials* **2016,** *28* (4), 1049-1057.

(11) Yang, J.; Tang, L.-S.; Bao, R.-Y.; Bai, L.; Liu, Z.-Y.; Yang, W.; Xie, B.-H.; Yang, M.-B., An Ice-templated Assembly Strategy To Construct Graphene Oxide/Boron Nitride Hybrid Porous Scaffolds in Phase Change Materials with Enhanced Thermal Conductivity and Shape Stability For Light–Thermal–Electric Energy Conversion. *J. Mater. Chem. A* **2016,** *4* (48), 18841-18851.

(12) Wu, H. C.; Kessler, M. R., Multifunctional Cyanate Ester Nanocomposites Reinforced by Hexagonal Boron Nitride after Noncovalent Biomimetic Functionalization. *ACS Appl. Mater. Interfaces* **2015,** *7* (10), 5915-5926.

(13) Su, Z.; Wang, H.; He, J.; Guo, Y.; Qu, Q.; Tian, X., Fabrication of Thermal Conductivity Enhanced Polymer Composites by Constructing an Oriented Three-Dimensional Staggered Interconnected Network of Boron Nitride Platelets and Carbon Nanotubes. *ACS Appl. Mater. Interfaces* **2018,** *10* (42), 36342-36351.

(14) Yao, Y.; Sun, J.; Zeng, X.; Sun, R.; Xu, J.-B.; Wong, C.-P., Construction of 3D Skeleton for Polymer Composites Achieving a High Thermal Conductivity. *Small* **2018,** *14* (13), 1704044.

(15) Kholmanov, I.; Kim, J.; Ou, E.; Ruoff, R. S.; Shi, L., Continuous Carbon Nanotube-Ultrathin Graphite Hybrid Foams for Increased Thermal Conductivity and Suppressed Subcooling in Composite Phase Change Materials. *ACS Nano* **2015,** *9* (12), 11699-11707.

(16) Nagaoka, S.; Jodai, T.; Kameyama, Y.; Horikawa, M.; Shirosaki, T.; Ryu, N.; Takafuji, M.; Sakurai, H.; Ihara, H., Cellulose/Boron Nitride Core–Shell Microbeads Providing High Thermal Conductivity for Thermally Conductive Composite Sheets. *RSC Adv.* **2016,** *6* (39), 33036-33042.

(17) Zhi, C.; Bando, Y.; Tang, C.; Kuwahara, H.; Golberg, D., Large-Scale Fabrication of Boron Nitride Nanosheets and Their Utilization in Polymeric Composites with Improved Thermal and Mechanical Properties. *Adv. Mater.* **2009,** *21* (28), 2889-2893.

(18) Guo, Y.; Lyu, Z.; Yang, X.; Lu, Y.; Ruan, K.; Wu, Y.; Kong, J.; Gu, J., Enhanced Thermal Conductivities and Decreased Thermal Resistances of

Functionalized Boron Nitride/Polyimide Composites. *Composites, Part B* **2019,** *164*, 732-739.

(19) Zhan, Y.; Long, Z.; Wan, X.; Zhan, C.; Zhang, J.; He, Y., Enhanced Dielectric Permittivity and Thermal Conductivity of Hexagonal Boron Nitride/Poly(Arylene Ether Nitrile) Composites through Magnetic Alignment and Mussel Inspired Co-Modification. *Ceramics International* **2017,** *43* (15), 12109-12119.

(20) Yuan, C.; Duan, B.; Li, L.; Xie, B.; Huang, M.; Luo, X., Thermal Conductivity of Polymer-Based Composites with Magnetic Aligned Hexagonal Boron Nitride Platelets. *ACS Appl. Mater. Interfaces* **2015,** *7* (23), 13000-13006.

(21) Lin, Z.; Liu, Y.; Raghavan, S.; Moon, K.-s.; Sitaraman, S. K.; Wong, C.-p., Magnetic Alignment of Hexagonal Boron Nitride Platelets in Polymer Matrix: Toward High Performance Anisotropic Polymer Composites for Electronic Encapsulation. *ACS Appl. Mater. Interfaces* **2013,** *5* (15), 7633-7640.

(22) Hu, J.; Huang, Y.; Yao, Y.; Pan, G.; Sun, J.; Zeng, X.; Sun, R.; Xu, J.-B.; Song, B.; Wong, C.-P., Polymer Composite with Improved Thermal Conductivity by Constructing a Hierarchically Ordered Three-Dimensional Interconnected Network of BN. *ACS Appl. Mater. Interfaces* **2017,** *9* (15), 13544-13553.

(23) Xiao, C.; Tang, Y.; Chen, L.; Zhang, X.; Zheng, K.; Tian, X., Preparation of Highly Thermally Conductive Epoxy Resin Composites via Hollow Boron Nitride Microbeads with Segregated Structure. *Composites, Part A* **2019,** *121*, 330-340.

(24) Han, W.; Bai, Y.; Liu, S.; Ge, C.; Wang, L.; Ma, Z.; Yang, Y.; Zhang, X., Enhanced Thermal Conductivity of Commercial Polystyrene Filled With Core-Shell Structured BN@PS. *Composites, Part A* **2017,** *102*, 218-227.

(25) Xiao, C.; Chen, L.; Tang, Y. L.; Zhang, X.; Zheng, K.; Tian, X. Y., Enhanced Thermal Conductivity of Silicon Carbide Nanowires (Sicw)/Epoxy Resin Composite with Segregated Structure. *Composites, Part A* **2019,** *116*, 98-105.

(26) Kinoshit, K.; Matsunag, N.; Hiraoka, M.; Yanagimoto, H.; Minami, H., Preparation of Boron Nitride and Polystyrene/Boron Nitride Composite Particles by Dehydrogenation in Ionic Liquids. *RSC Adv.* **2014,** *4* (17), 8605-8611.

(27) Kim, K.; Kim, J., Core-Shell Structured BN/PPS Composite Film for High Thermal Conductivity with Low Filler Concentration. *Compo. Sci. Technol.* **2016,** *134*, 209-216.

(28) Jiang, Y.; Liu, Y.; Min, P.; Sui, G., BN@PPS Core-Shell Structure Particles and their 3D Segregated Architecture Composites with High Thermal Conductivities. *Compos. Sci. Technol.* **2017,** *144*, 63-69.

(29) Pickering, S. U., Emulsions. *Journal of the Chemical Society* **1907,** *91*, 2001-2021.

(30) Tang, M.; Wang, X.; Wu, F.; Liu, Y.; Zhang, S.; Pang, X.; Li, X.; Qiu, H., Au Nanoparticle/Graphene Oxide Hybrids as Stabilizers for Pickering Emulsions and Au Nanoparticle/Graphene Oxide@Polystyrene Microspheres. *Carbon* **2014,** *71*, 238-248.

(31) Ortiz, D. G.; Pochat-Bohatier, C.; Cambedouzou, J.; Balme, S.; Bechelany, M.; Miele, P., Inverse Pickering Emulsion Stabilized by Exfoliated Hexagonal-Boron Nitride (h-BN). *Langmuir* **2017,** *33* (46), 13394-13400.

(32) Moghaddam, S. Z.; Sabury, S.; Sharif, F., Dispersion ff rGO in Polymeric Matrices by Thermodynamically Favorable Self-Assembly of GO at Oil-Water Interfaces. *RSC Adv.* **2014,** *4* (17), 8711-8719.

(33) Huang, X.; Sun, B.; Su, D.; Zhao, D.; Wang, G., Soft-Template Synthesis of 3D Porous Graphene Foams with Tunable Architectures for Lithium–O2 Batteries and Oil Adsorption Applications. *J. Mater. Chem. A* **2014,** *2* (21), 7973-7979.

(34) Xie, P.; Ge, X.; Fang, B.; Li, Z.; Liang, Y.; Yang, C., Pickering Emulsion Polymerization of Graphene Oxide-Stabilized Styrene. *Colloid and Polymer Science* **2013,** *291* (7), 1631-1639.

(35) Gonzalez-Ortiz, D.; Pochat-Bohatier, C.; Gassara, S.; Cambedouzou, J.; Bechelany, M.; Miele, P., Development of Novel H-BNNS/PVA Porous Membranes via Pickering Emulsion Templating. *Green Chemistry* **2018,** *20* (18), 4319-4329.

(36) Chen, S.; Xu, R.; Liu, J.; Zou, X.; Qiu, L.; Kang, F.; Liu, B.; Cheng, H.-M., Simultaneous Production and Functionalization of Boron Nitride Nanosheets by Sugar-Assisted Mechanochemical Exfoliation. *Adv. Mater.* **2019,** *31* (10), 1804810-1804810.

(37) Ortiz, D. G.; Pochat-Bohatier, C.; Cambedouzou, J.; Bechelany, M.; Miele, P., Pickering Emulsions Stabilized with Two-Dimensional (2D) Materials: A

Comparative Study. *Colloids and Surfaces A-Physicochemical and Engineering Aspects* **2019,** *563*, 183-192.

(38) Lin, Y.; Connell, J. W., Advances in 2D Boron Nitride Nanostructures: Nanosheets, Nanoribbons, Nanomeshes, and Hybrids with Graphene. *Nanoscale* **2012,** *4* (22), 6908-6939.

(39) Annan, W. S.; Fairhead, M.; Pereira, P.; van der Walle, C. F., Emulsifying Performance of Modular Beta-Sandwich Proteins: the Hydrophobic Moment and Conformational Stability. *Protein Eng. Des. Sel.* **2006,** *19* (12), 537-45.

(40) Binks, B. P., Particles as Surfactants—Similarities and Differences. *Current Opinion in Colloid & Interface Science* **2002,** *7* (1), 21-41.

(41) Li, H.; Zeng, X. C., Wetting and Interfacial Properties of Water Nanodroplets in Contact with Graphene and Monolayer Boron-Nitride Sheets. *ACS Nano* **2012,** *6* (3), 2401-2409.

(42) Annamalai, M.; Gopinadhan, K.; Han, S. A.; Saha, S.; Park, H. J.; Cho, E. B.; Kumar, B.; Patra, A.; Kim, S.-W.; Venkatesan, T., Surface Energy and Wettability of Van Der Waals Structures. *Nanoscale* **2016,** *8* (10), 5764-5770.

(43) Wang, J.; Zhang, D.; Zhang, Y.; Cai, W.; Yao, C.; Hu, Y.; Hu, W., Construction of Multifunctional Boron Nitride Nanosheet towards Reducing Toxic Volatiles (CO And HCN) Generation and Fire Hazard of Thermoplastic Polyurethane. *Journal of Hazardous Materials* **2019,** *362*, 482-494.

(44) Yin, C.-G.; Ma, Y.; Liu, Z.-J.; Fan, J.-C.; Shi, P.-H.; Xu, Q.-J.; Min, Y.-L., Multifunctional Boron Nitride Nanosheet/Polymer Composite Nanofiber Membranes. *Polymer* **2019,** *162*, 100-107.

(45) Maleki, M.; Beitollahi, A.; Javadpour, J.; Yahya, N., Dual Template Route for the Synthesis of Hierarchical Porous Boron Nitride. *Ceramics International* **2015,** *41* (3), 3806-3813.

(46) Thakur, V. K.; Yan, J.; Lin, M. F.; Zhi, C. Y.; Golberg, D.; Bando, Y.; Sim, R.; Lee, P. S., Novel Polymer Nanocomposites from Bioinspired Green Aqueous Functionalization of BNNTs. *Polymer Chemistry* **2012,** *3* (4), 962-969.

(47) Gou, G. Y.; Pan, B. C.; Shi, L., Noncovalent Functionalization of BN Nanotubes with Perylene Derivative Molecules: An ab Initio Study. *ACS Nano* **2010,** *4* (3), 1313-1320.

(48) Wang, X.; Wu, P., Preparation of Highly Thermally Conductive Polymer Composite at Low Filler Content via a Self-Assembly Process between Polystyrene Microspheres and Boron Nitride Nanosheets. *ACS Appl. Mater. Interfaces* **2017,** *9* (23), 19934-19944.

(49) Yu, J.; Huang, X.; Wu, C.; Wu, X.; Wang, G.; Jiang, P., Interfacial Modification of Boron Nitride Nanoplatelets For Epoxy Composites With Improved Thermal Properties. *Polymer* **2012,** *53* (2), 471-480.

(50) Kim, K.; Ju, H.; Kim, J., Vertical Particle Alignment of Boron Nitride and Silicon Carbide Binary Filler System for Thermal Conductivity Enhancement. *Compo. Sci. Technol.* **2016,** *123*, 99-105.

(51) Leng, X.; Xiao, C.; Chen, L.; Su, Z.; Zheng, K.; Zhang, X.; Tian, X., An Efficient Approach for Constructing 3-D Boron Nitride Networks with Epoxy Composites to form Materials with Enhanced Thermal, Dielectric, and Mechanical Properties. *High Performance Polymers* **2019,** *31* (3), 350-358.

(52) Cui, J.; Zhou, S., Facile Fabrication of Highly Conductive Polystyrene/Nanocarbon Composites with Robust Interconnected Network via Electrostatic Attraction Strategy. *J. Mater. Chem. C.* **2018,** *6* (3), 550-557.

(53) Yu, S.; Hing, P.; Hu, X., Thermal Conductivity of Polystyrene–Aluminum Nitride Composite. *Composites, Part A* **2002,** *33* (2), 289-292.

(54) Jiang, X. L.; Ma, P. F.; You, F.; Yao, C.; Yao, J. L.; Liu, F. J., A Facile Strategy for Modifying Boron Nitride and Enhancing its Effect on the Thermal Conductivity of Polypropylene/Polystyrene Blends. *RSC Adv.* **2018,** *8* (56), 32132-32137.

(55) Wu, G.; Wang, Y.; Wang, K.; Feng, A., The Effect of Modified Aln on the Thermal Conductivity, Mechanical and Thermal Properties of Aln/Polystyrene Composites. *RSC Adv.* **2016,** *6* (104), 102542-102548.

(56) Huang, X.; Wang, S.; Zhu, M.; Yang, K.; Jiang, P.; Bando, Y.; Golberg, D.; Zhi, C., Thermally Conductive, Electrically Insulating and Melt-Processable Polystyrene/Boron Nitride Nanocomposites Prepared by in Situ Reversible addition Fragmentation Chain Transfer Polymerization. *Nanotechnology* **2015,** *26* (1).

(57) Fang, L.; Wu, C.; Qian, R.; Xie, L.; Yang, K.; Jiang, P., Nano-Micro Structure of Functionalized Boron Nitride and Aluminum Oxide for Epoxy

Composites with Enhanced Thermal Conductivity and Breakdown Strength. *RSC Adv.* **2014,** *4* (40), 21010-21017.

Table of contents

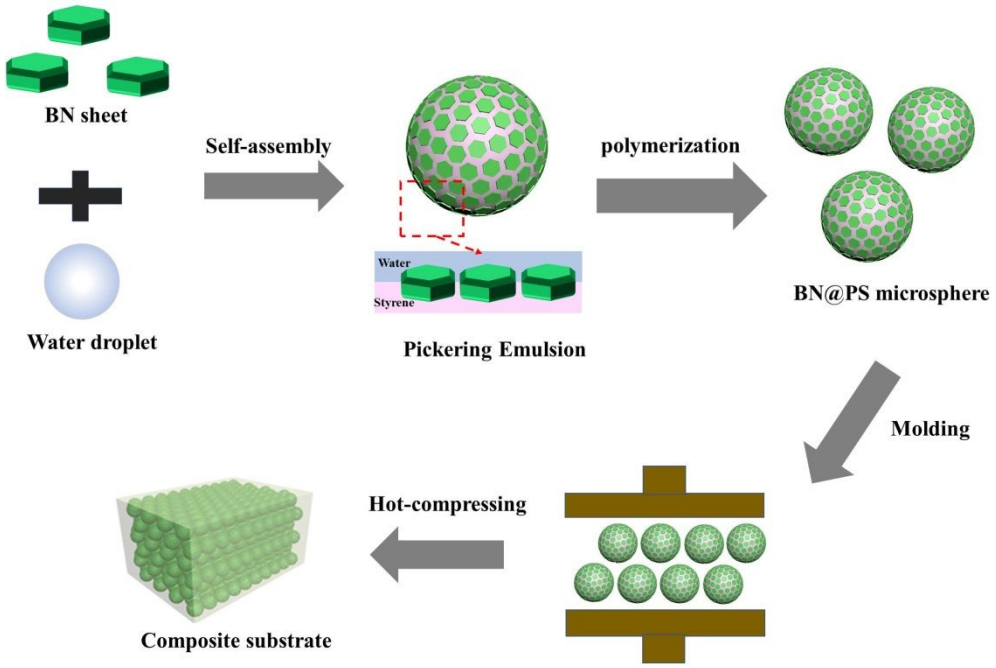

The Highly Thermally Conductive Polymer Composite is fabricated by Assembly of Boron Nitride at Oil Water Interface

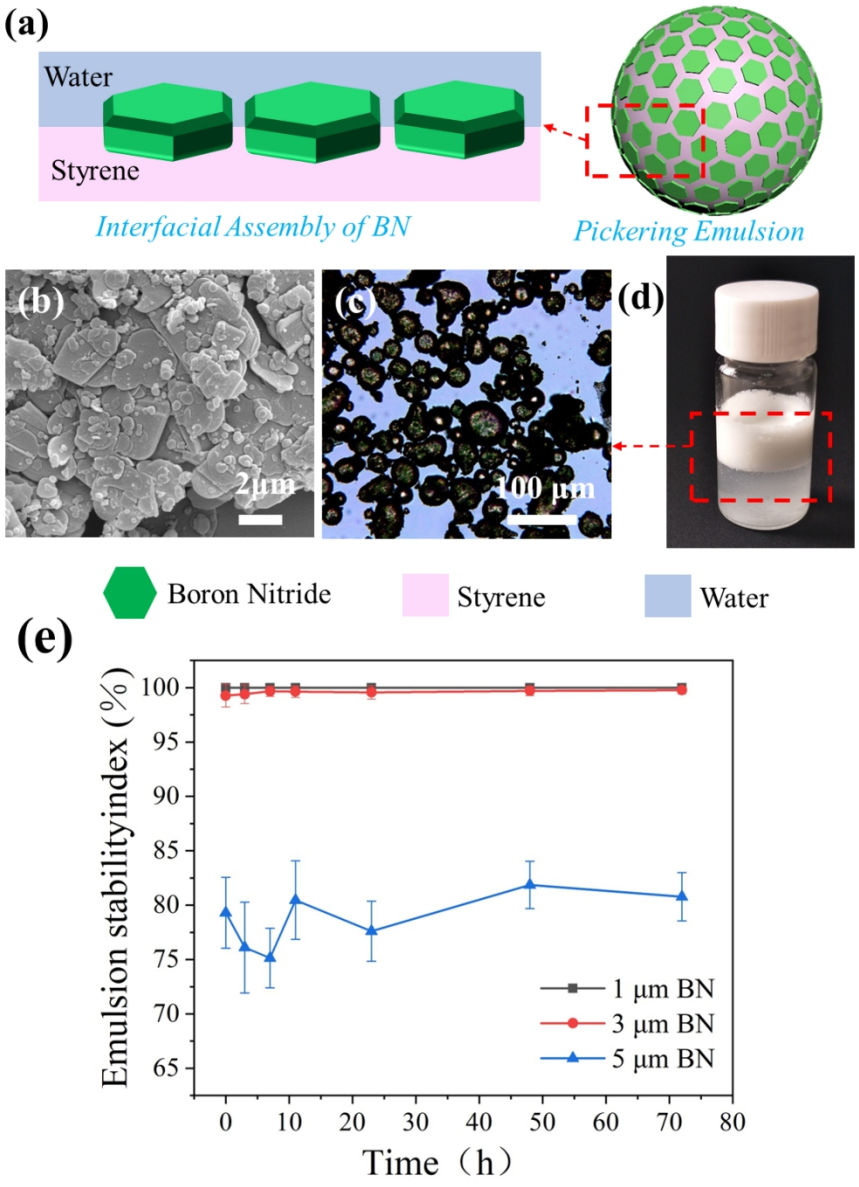

Fig. 1 (a) Schematic of Pickering emulsion, (b) SEM image of BN particles with mean size of 3 μm (c) the optical microscopy image of Pickering emulsions; (d) photograph of typical Pickering emulsion stabilized by BN ; and (e) Emulsion stability index (ESI) as a function of time for Pickering emulsion stabilized by BN particles.

191x262mm (150 x 150 DPI)

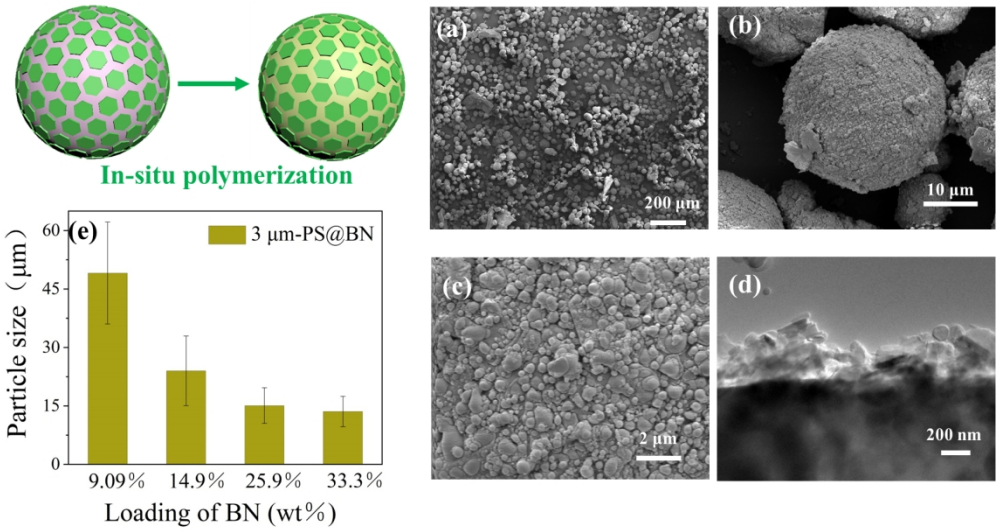

Fig. 2 The cartoon illustrates the formation of PS@BN microspheres from in-situ polymerization of Pickering emulsion. (a) SEM image of PS@BN microspheres stabilized by 3 μm BN sheets. SEM images of a typical PS@BN microsphere with (b) low and (c) high magnifications; (d) TEM image, (e) particle size distribution

316x167mm (150 x 150 DPI)

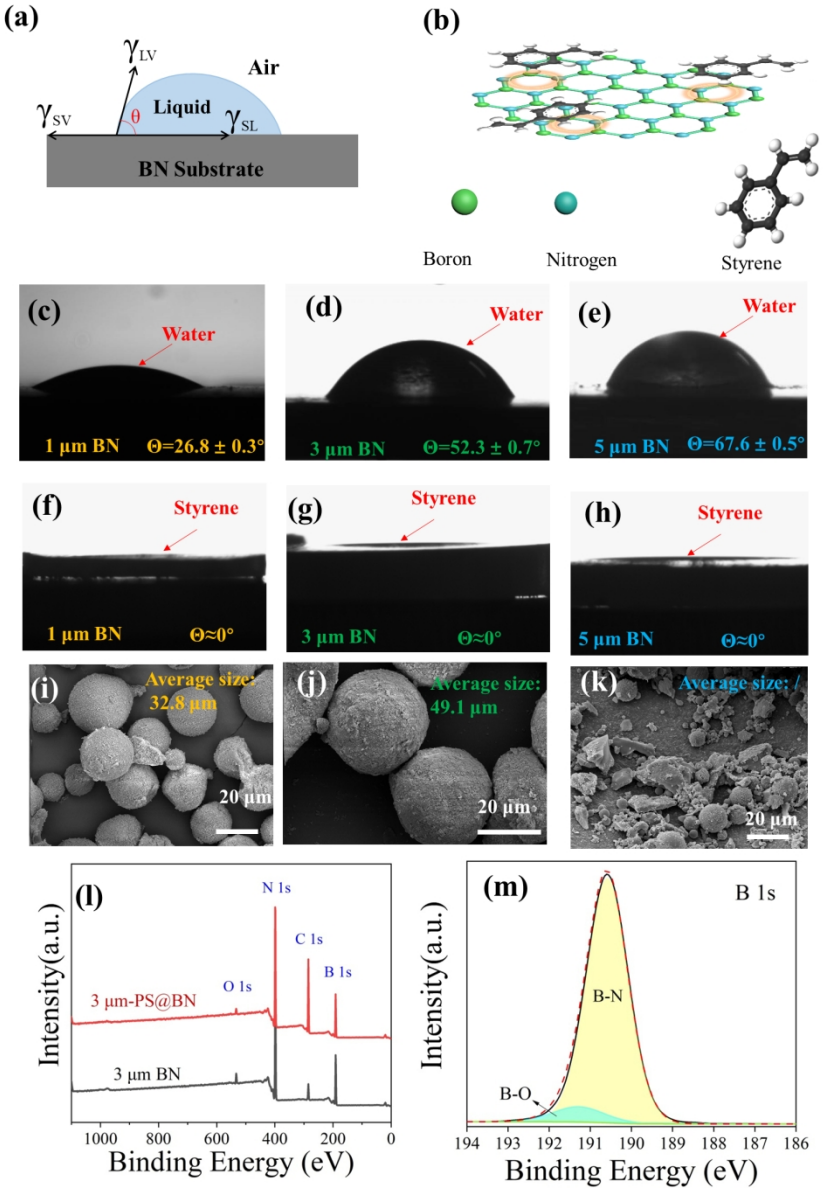

Fig.3 (a) Schematic configuration of contact angle measurements; (b) schematic illustration of interaction between BN and PS, the orange ring denotes the π-π stacking effects; (c-e) contact angles of water droplet on the tablets made of BN with various sizes; (f-h) contact angles of styrene droplet on the tablets made of BN with various sizes; SEM images of PS@BN microsphere obtained by BN sheets with mean size of (i)1 μm, (j) 3 μm and (k) 5 μm. (l) XPS spectra of the 3 μm BN and 3 μm-PS@BN microspheres; (m) B 1s high-resolution spectrum of 3 μm BN . The content of BN in feed was 9.09 wt% for the preparation of all the above samples.

274x384mm (150 x 150 DPI)

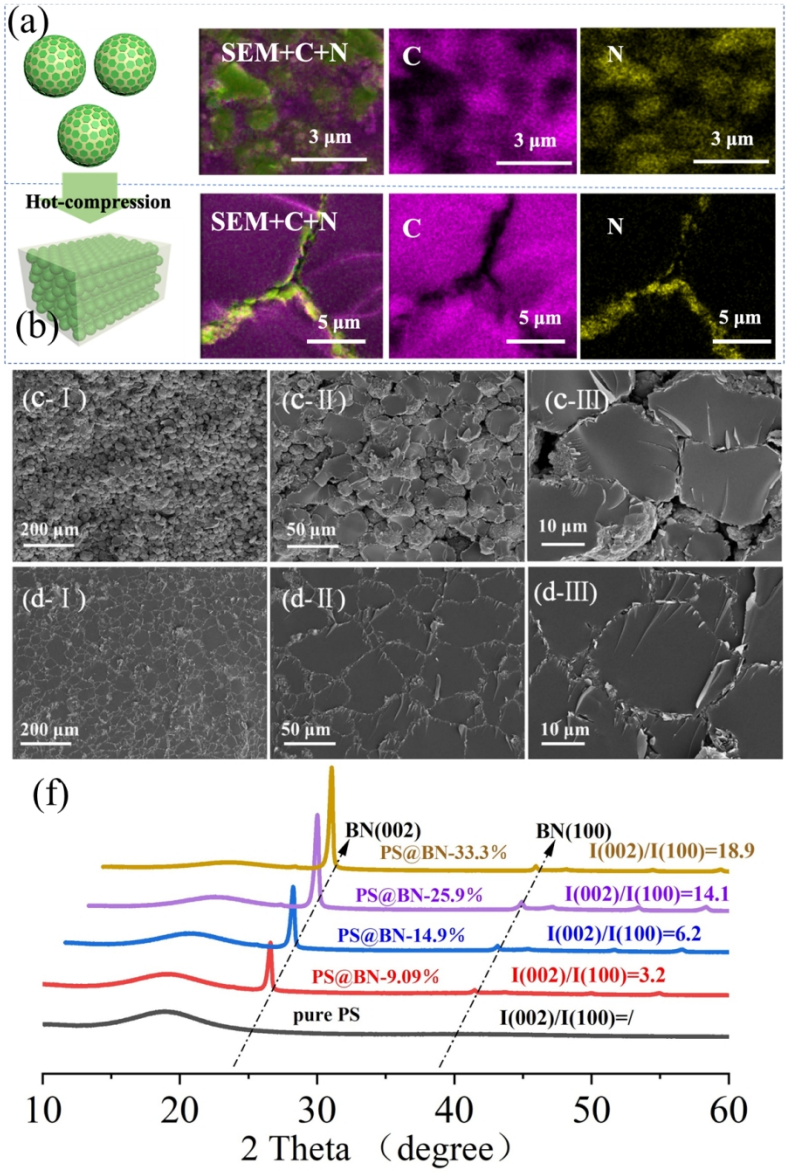

Fig. 4 EDS elemental mapping images of (a) the surface of PS@BN composite microspheres and (b) cross-section of composite substrate; cross-section SEM images of composite substrate under different conditions of hot-pressing: (c) 80℃, 25MPa; (d) 95℃, 25Mpa; Ⅰ, Ⅱ, Ⅲ represent the SEM at different magnifications, respectively; (f) XRD patterns of the composite substrates made from PS@BN microspheres with varies BN loadings.

205x302mm (150 x 150 DPI)

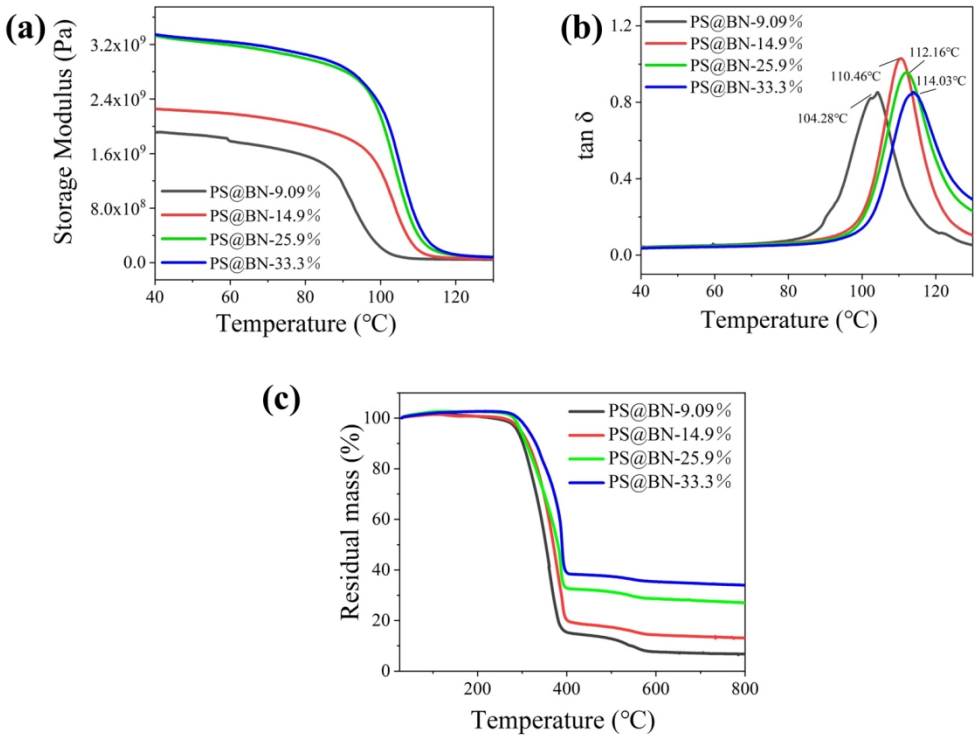

Fig. 5 Dynamic mechanical analysis (DMA) of the PS@BN composite substrates, (a) storage modulus and (b) loss tangent (tan δ) versus temperature of the composite substrates; (c) thermogravimetric analysis of PS@BN composite substrates with increased content of BN.

275x205mm (150 x 150 DPI)

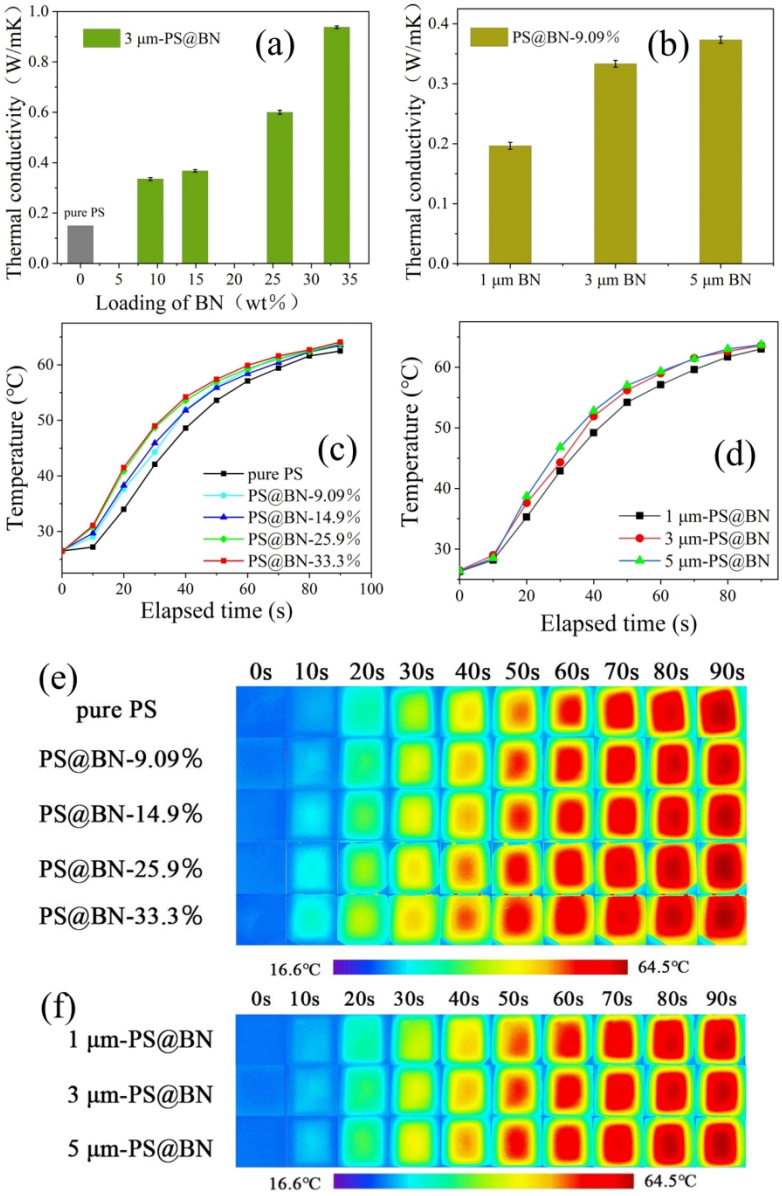

Fig. 6 (a) Thermal conductivity of composite substrate against the BN content; (b) thermal conductivity of composite substrate against the size of BN; surface temperature evolution with elapsed time of the composite made with different BN (c) loadings and (d) sizes; infrared images taken by each 10 seconds for the composite substrate made with different BN contents (e) and different BN sizes (f)

243x368mm (150 x 150 DPI)